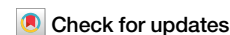


<https://doi.org/10.1038/s44323-025-00032-6>

Chronic circadian disruption alters cardiac function and glucose regulation in mice

Jenna E. J. Gearey^{1,2}, Melinda Wang^{1,2} & Michael C. Antle^{1,2,3}

Cardiometabolic disease is a leading cause of death worldwide. One factor that may contribute to the risk, onset, and severity of symptoms is disrupted circadian rhythms. Our study uses two strains of mice to further elucidate this relationship: healthy controls, and a mouse model of insulin resistance with short freerunning periods (~ 22.75 h) and enlarged hearts, raised in either a 24-h or 22.75-h LD cycle. Through glucose and insulin tolerance tests, routine electrocardiograms from one to four months old, and histology, we reveal worse cardiometabolic health outcomes for mice gestated and housed in a mismatched LD cycle compared to those in an LD cycle that matches their endogenous rhythm. This was characterized by heightened blood glucose levels following a glucose or insulin bolus, altered electrophysiological parameters of the cardiac waveform, and increased cardiomyocyte size. Circadian disruption due to work/social schedules or circadian-related disorders in people is often confounded with other unhealthy lifestyles. The present study demonstrates that circadian disruption on its own can lead to adverse health states.

Noncommunicable diseases are the leading cause of death worldwide, accounting for 80% of mortalities, with cardiovascular disease and metabolic diseases being within the top ten^{1,2}. One factor that affects the risk and onset of heart disease, diabetes, and obesity is disrupted circadian rhythms³. Such disruption occurs when there is a conflict between our endogenous circadian clock that is entrained to the solar day-night cycle, and our social clock that dictates the timing of our behaviors such as work, school, and leisure activities. Conflict and disruption may result from nighttime light exposure, chronic jetlag, social jetlag, rotating shiftwork or persistent night shifts, circadian rhythm sleep-wake disorders, and even living in the western portion of a time zone^{3–8}.

The master circadian clock in the suprachiasmatic nucleus is entrained to our day-night cycle, and relays phase information to peripheral oscillators throughout the rest of the body through neurohumoral communication^{9–11}. This regulates daily fluctuations of cardiometabolic parameters such as heart rate, blood pressure, ion homeostasis, electrophysiology, contractility, hormonal signaling, and metabolic gene transcription^{12–16}. Accordingly, disruptions within the circadian system through misalignment between rhythmic behavior and the day/night cycle have consequences on cardiometabolic health^{7,17–20}. Specifically, shift-workers are 23% more likely to be obese, have 14% higher rates of diabetes, and 30% more likely to have hypertension^{5,7}. However, these misaligned lifestyles are often accompanied by changes in quality of diet and exercise that could differentially affect one's

risk of disease, making it difficult to separate the effects of circadian disruption from the effects of the lifestyle on disease progression^{5,7,21}.

By using animal models, it is possible to disentangle the contribution of circadian disruption on disease state from other confounding variables. The relationship between cardiovascular disease has been well-established in adult hamsters using casein kinase 1 ϵ (*Tau*) mutant hamsters with 22-h freerunning periods (FRP)²². When 22-h heterozygotes mutants are raised on a 24-h LD cycle, it results in cardiac hypertrophy, interstitial fibrosis, impaired contractility, and reduced lifespans by 17 months old. However, when these hamsters are housed on a 22-h LD cycle that matches their FRP, their heart function is rescued, and their lifespan is comparable to controls. Circadian misalignment also leads to cardiometabolic disease in adult wildtype mice raised on either a 22.5-h LD cycle or 27-h LD cycle, compared to a normal 24-h day^{23,24}. In both misaligned LD cycles, mice show decreased metabolic efficiency (e.g. lower body weight, increased food intake, increased energy expenditure, higher oxygen consumption, increase in respiratory exchange rate and carbohydrate oxidation) and disrupted cardiac function^{23–27}. Even just perinatal circadian disruption can alter behavioral, cardiac and metabolic properties, leading to altered behavior, and altered glucose tolerance and heart rate variability when rodents reached adulthood^{28–30}. Extreme circadian disruption due to rearing mice in an extremely short 8:8 LD cycle initiated during gestation leads to glucose intolerance³¹, heavier body weight, higher fasting blood glucose levels,

¹Department of Psychology, University of Calgary, Calgary, AB, Canada. ²Hotchkiss Brain Institute, University of Calgary, Calgary, AB, Canada. ³Department of Physiology and Pharmacology, Cumming School of Medicine, University of Calgary, Calgary, AB, Canada. ✉e-mail: antlem@ucalgary.ca

pathological cardiac remodeling and cardiac arrhythmia³². Taken together, these studies demonstrate that circadian disruption adversely affects cardiometabolic health.

Like in humans, there can be many underlying causes of cardiometabolic disease. The BTBR mouse strain is prone to several adverse health conditions. These mice show early insulin resistance, higher body weight, routine barbering, perseverance and altered corticosterone levels^{33–35}. From observations in our lab, they also exhibit cardiac hypertrophy and shorter lifespans. Importantly, BTBR mice also have extremely short FRPs (22.74 ± 0.10 h)³⁶. Given the chronic misalignment between BTBRs FRP and the normal 24-h LD cycle used in animal facilities, the aim of this experiment is to (1) determine how much of the BTBR mouse altered cardiometabolic physiology is due to circadian misalignment, and (2) to explore the onset of disease in typical healthy mouse strain (C57BL/6 J, B6) exposed to early life circadian misalignment. It is hypothesized that (1) BTBR mice and (2) B6 mice will experience worse cardiometabolic health outcomes when conceived and housed in a misaligned LD cycle. Specifically, it is predicted that misaligned mice will show cardiac hypertrophy, cardiac fibrosis, prolonged RR, QTc, and JT intervals, and highest blood glucose levels following an injection of glucose or insulin.

Results

Physical features

Given that circadian misalignment during gestation has been associated with poorer outcomes in adulthood, we raised two different mouse strains from conception onwards under different LD cycles that either matched or mismatched their respective average FRPs³⁶ (Fig. 1). We first asked if the overall physical differences observed in BTBR mice (greater body weight and heart size) was a consequence of being raised in a standard 12:12LD cycle that was longer than their average FRP of 22.75 h, and if similar health consequences could be caused in B6 mice raised in similarly mismatched LD cycle (11.375:11.375LD). Body weight increased steadily between one month and four months of age in BTBR and B6 mice ($F_{(3, 300)} = 901.59$, $p < 0.001$, $\omega_p = 0.24$; Supplementary Table 1). Additionally, males were significantly heavier than females ($F_{(2, 100)} = 76.39$, $p < 0.001$, $\omega_p = 0.42$). Together, there was an interaction between LD cycle and age ($F_{(1.52, 152.28)} = 9.08$, $p < 0.001$, $\omega_p = 0.03$), with BTBR mice from the 22.75-h LD cycle ($p < 0.001$) and the 24-h LD cycle ($p < 0.001$) weighing more than B6 mice from the 24-h LD cycle (Fig. 2).

A subset of mice were retained until six months of age to collect hearts for histology. By six months of age, BTBR mice had significantly greater bodyweights than B6 mice ($F_{(1,74)} = 14.59$, $p < 0.001$, $\omega_p = 0.14$, Fig. 3B), and males were significantly larger than females ($F_{(1,74)} = 21.88$, $p < 0.001$, $\omega_p = 0.20$). Weight was not significantly altered by LD cycle ($F_{(1,74)} = 0.44$, $p = 0.507$). None of the interactions were significant.

We next examined heart size. BTBR mice have much larger hearts overall (Fig. 3A), but given their large body, we normalized heart size for body size for analysis. At six months old BTBR mice had significantly larger normalized heart weight (Fig. 3C; $F_{(1,74)} = 28.97$, $p < 0.001$, $\omega_p = 0.25$), however, this was not significantly affected by LD cycle ($F_{(1,74)} = 2.07$, $p = 0.154$). There were no other main effects or interactions. We next used Mason Trichrome Stain to examine heart histology. At six months of age, there were no obvious difference in fibrosis (Fig. 2E–L). However, there were significant differences found in the cross-sectional area (CSA) of cardiomyocytes between strains (Fig. 3D; $F_{(1,34)} = 23.22$, $p < 0.001$, $\omega_p = 0.35$). Specifically, cardiomyocyte size was larger in mice from the mismatched LD cycle compared to the matched LD cycle for both strains ($F_{(1,34)} = 5.75$, $p < 0.001$, $\omega_p = 0.35$), with BTBR mice showing the most notable difference in cell size (Fig. 3). No significant interactions were found.

Electrocardiogram (ECG) parameters and measurements

Next we explored if a mismatched LD cycle altered cardiac function as determined by an electrocardiogram. To explore this possibility, we next examined changes to ECG parameters recorded at three timepoints: one, two and four months of age. Given the difference in heart and cardiomyocyte size, BTBR and B6 were analyzed separately. ECG parameters were manually quantified and compared between LD cycles and sex. Cardiac parameters of interest are heart rate, RR interval, QTc interval, JT interval, and R amplitude.

BTBR mice exhibited a slowing in heart rate as they aged ($F_{(2,118)} = 14.02$, $p < 0.001$, $\omega_p = 0.10$, Fig. 4B), with the heart rate at one month being faster than at later time points ($p < 0.05$). Furthermore, females had slower heart rates than males ($F_{(1,59)} = 4.30$, $p = 0.042$, $\omega_p = 0.05$). These main effects were modulated by a significant LD cycle by sex by age interaction ($F_{(2,118)} = 3.85$, $p = 0.024$, $\omega_p = 0.02$) where heart rates tended to be lower in the mismatch LD cycle, particularly at later ages and more so in male mice ($p < 0.01$).

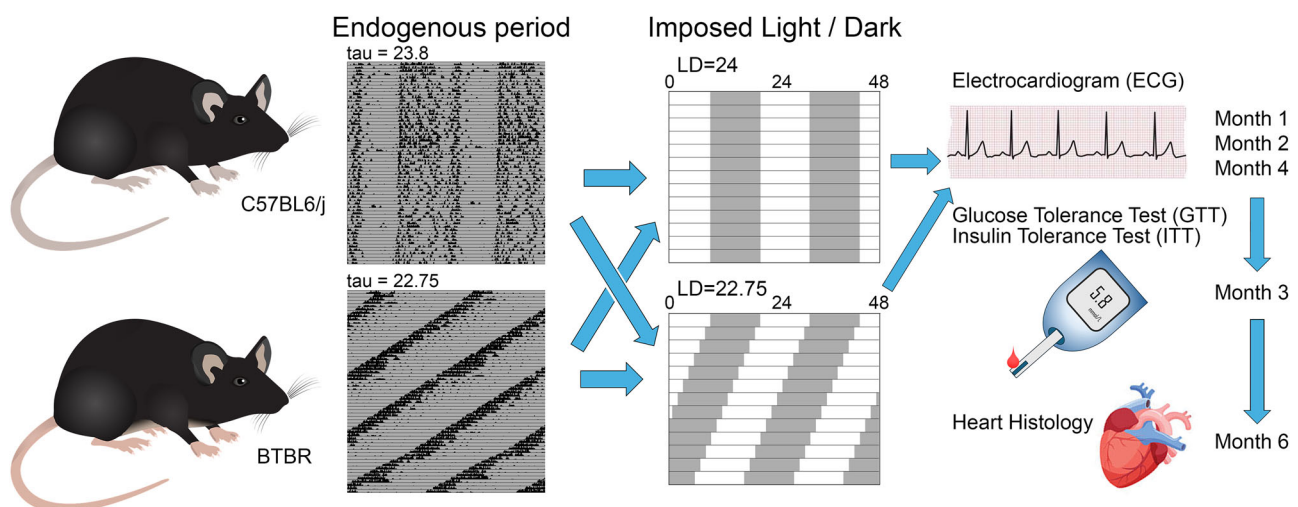


Fig. 1 | A schematic of our methodology highlighting strains of mice, light/dark (LD) cycles, and measurements. B6 mice (top mouse) and BTBR mice (bottom mouse), display different endogenous periods in constant conditions (respective actograms). Each strain was bred in both LD cycles: one that matched and one that did not match their endogenous rhythm (LD = 24, LD = 22.74). Over the first six

months of life, electrocardiograms were ran at one-, two-, and four-months-old. Mice were randomly assigned to a GTT or ITT at three months old. At six months, they were perfused and hearts were collected for histology. Mouse graphic from <https://creazilla.com/media/clipart/19072/lab-mouse> used under CC0 1.0 licence.

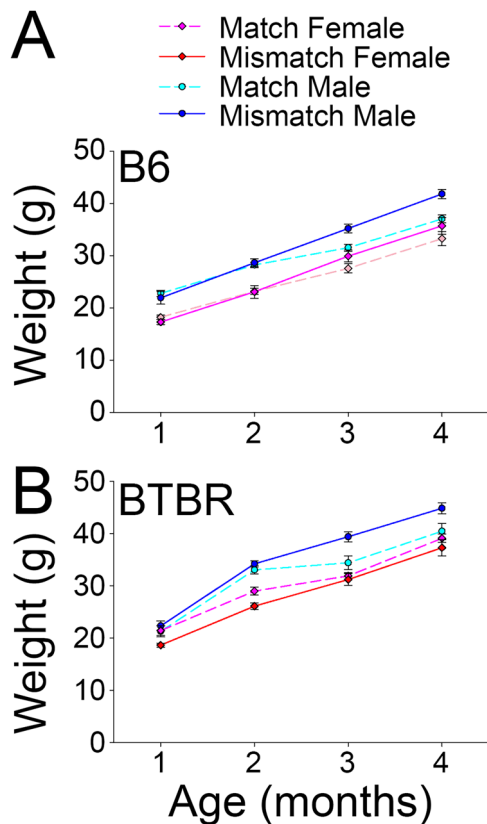


Fig. 2 | Weight increase over time in B6 and BTBR raised in different LD cycles. Changes in bodyweight in B6 (A) and BTBR (B) mice between LD cycles. Weight was tracked over the first four months. BTBR mice showed significantly larger body weight compared to B6 mice in a matched LD cycle when raised in a matched LD cycle ($p < 0.001$) or mismatched LD cycle ($p < 0.001$).

In B6 mice, while heart rates also tended to be slightly higher at earlier ages, this pattern was not significant ($F_{(2,118)} = 2.69$, $p = 0.074$, Fig. 4A). Additionally, while heart rates tended to be lower in the mismatch LD cycle at later ages, this interaction was also not significant ($F_{(2,82)} = 2.97$, $p = 0.057$).

We next examined the RR interval. RR interval changed in BTBR mice over time ($F_{(2,118)} = 16.73$, $p < 0.001$, $\omega_p = 0.12$, Fig. 4E) being shortest at one month of age and longest at two months of age. RR interval was also longer in female BTBR mice ($F_{(1,59)} = 6.23$, $p = 0.015$, $\omega_p = 0.08$). RR intervals were slightly longer in the mismatched LD cycle, although this difference was not significant ($F_{(1,59)} = 2.91$, $p = 0.093$). The lack of a main effect here might have been influenced by a weak but non-significant three-way interaction between sex, age, and LD cycle ($F_{(2,118)} = 3.00$, $p = 0.053$, $\omega_p = 0.02$).

B6 mice displayed significant differences in the length of the RR interval between LD cycles overtime ($F_{(2,82)} = 3.64$, $p = 0.031$, $\omega_p = 0.03$), with B6 mice in the misaligned LD cycle showing significantly longer RR intervals at four months of age compared to those housed in a normal LD cycle (Fig. 4D; $p = 0.004$). None of the other main effects or interactions were significant.

As alterations in RR interval could indicate altered heart function, we next examined several more specific ECG measures. We first examined the heart-rate corrected QT interval (QTc). A prolonged QTc interval is associated with increased risk of ventricular arrhythmias and cardiac hypertrophy^{23,27,37} while a shortened QTc is associated with a variety of heart conditions, including sudden cardiac death³⁷. BTBR mice housed in the mismatched LD cycle had shorter QTc intervals (Fig. 4H; $F_{(1,59)} = 9.11$, $p = 0.004$, $\omega_p = 0.12$). QTc was longest at one month of age, and shortest at two months of age ($F_{(2,118)} = 8.56$, $p < 0.001$, $\omega_p = 0.06$). Males had longer QTc intervals than females ($F_{(1,59)} = 33.80$, $p = 0.004$, $\omega_p = 0.11$). There were no significant interactions between sex, age and LD cycle.

With B6 mice, there was a significant shortening of QTc as they got older ($F_{(2,82)} = 3.68$, $p = 0.029$, $\omega_p = 0.03$, Fig. 4G). Although female mice decreased consistently overtime, this interaction with age was not significant ($F_{(2,82)} = 3.01$, $p = 0.055$). LD cycle did not significantly alter QTc interval in the B6 mice ($F_{(1,41)} = 0.42$, $p = 0.522$, $\omega_p = .00$). There were no other main effects or interactions for QTc in B6 mice.

We next examined if the treatments altered the JT interval. Because the J wave accounts for 90% of the repolarization of the murine heart, abnormalities in this segment have been associated with heart failure and aging^{25,26}. The mismatched LD cycle led to a significant decrease in the JT interval in BTBR mice ($F_{(1,59)} = 10.96$, $p = 0.002$, $\omega_p = 0.14$), although this difference was only observed at the one month of age timepoint (age x LD cycle interaction, $F_{(2,118)} = 13.63$, $p < 0.001$, $\omega_p = 0.10$; Fig. 4K), after which the JT intervals normalized. Additionally, females had a shorter JT interval than males ($F_{(1,59)} = 33.479$, $p = 0.033$, $\omega_p = 0.06$). There were no other main effects or interactions for JT in the BTBR mice.

B6 mice housed in the mismatched LD cycle had a longer JT interval than those in the matched 24 h LD cycle ($F_{(1,41)} = 9.29$, $p = 0.004$, $\omega_p = 0.16$, Fig. 4J) at one month old ($p < 0.001$). There was no main effect of sex or age, and no further interactions.

We then looked at R amplitude as it has been shown to increase during development and correlate with normalized heart weight^{27,38}. Female BTBRs had the largest R wave amplitudes (main effect of sex, $F_{(1,59)} = 7.80$, $p = 0.007$, $\omega_p = 0.10$; Fig. 4N), although this was only observed when they were in the matched LD cycle (sex x LD cycle interaction, $F_{(1,59)} = 13.74$, $p < 0.001$, $\omega_p = 0.17$). There was a main effect of session, with most groups showing an increase in R amplitude as they aged, apart from females in the short LD cycle ($F_{(2,118)} = 4.78$, $p = 0.010$, $\omega_p = 0.04$). The R amplitude of these females decreased overtime (LD cycle by sex by session interaction; $F_{(2,118)} = 3.28$, $p = 0.041$). However, these last two p values should be interpreted cautiously given violations to normality.

The R wave amplitude in B6 mice significantly increased with age ($F_{(2,82)} = 3.47$, $p = 0.036$, $\omega_p = 0.03$, Fig. 4M). There was no significant effect of LD cycle ($F_{(1,41)} = 0.27$, $p = 0.605$), nor any significant interaction with LD cycle and the other variables.

Given that cardiac function can vary with bodyweight, these same ECG measures were also analyzed when normalized for bodyweight. Effects of LD cycle persisted when normalized in this fashion. These analyses are presented in Supplementary Fig. 4 and Supplementary Table 2.

Intraperitoneal glucose and insulin tolerance tests

Circadian disruption has been associated with development of insulin resistance and delayed glucose clearance^{39,40}. Because BTBR mice have been used as a mouse model that develops insulin resistance, we next asked if being raised in a LD cycle that was mismatched with their own endogenous circadian period contributed to a diabetic phenotype characterized by poorer responses to a glucose or insulin challenge.

Fasted mice had a baseline blood-glucose level measured prior to receiving a bolus of glucose (2 g/kg). They then had their glucose levels assessed at 15-, 30-, 60-, and 120-min after the injection. Based on these measures, an Area Under the Curve (AUC) was calculated for blood-glucose levels.

Results from GTT tests revealed a significant interaction between strain and LD cycle ($F_{(1,51)} = 28.89$, $p < 0.001$, $\omega_p = 0.32$; Fig. 5A) and sex and LD cycle ($F_{(1,51)} = 6.25$, $p = 0.016$, $\omega_p = 0.08$). Male B6 mice show poorer glucose clearance in a misaligned LD cycle compared to other B6 mice ($p < 0.001$), and misaligned female B6 mice displaying significantly larger AUCs than female B6 mice in raised in a normal LD cycle ($p < 0.01$). Male BTBR mice raised in a misaligned LD cycle had larger AUCs than females in a misaligned LD cycle ($p < 0.01$), but not males in a matched LD cycle ($p = 0.212$). There were no differences found between BTBR females ($p = 0.289$).

Finally, we examined clearance of glucose from the blood following administration of insulin. Fasted mice had a baseline blood-glucose level measured prior to receiving a bolus of insulin (0.75IU/kg). They then had their glucose levels assessed at 15-, 30-, 60-, and 120-min after the injection.

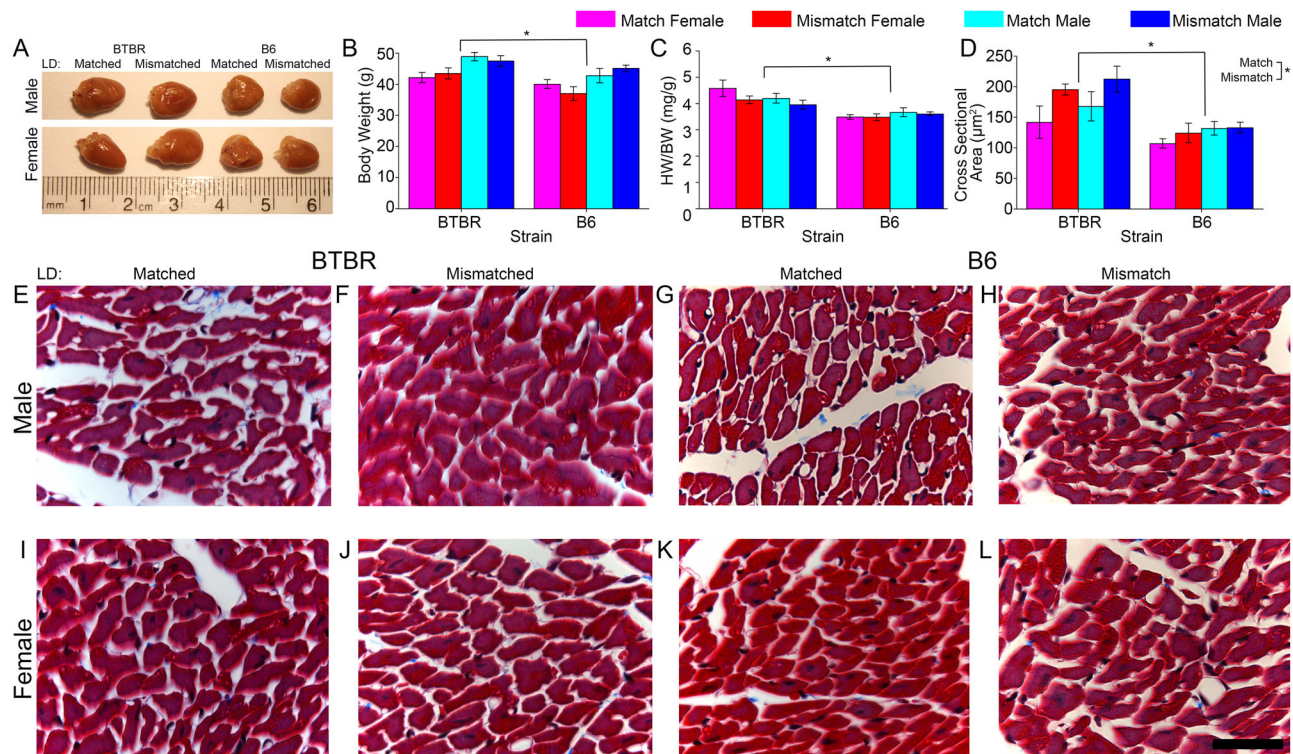


Fig. 3 | Cardiac anatomy and histology in BTBR and B6 mice raised in different LD cycles. BTBR mice weighed more than B6 mice at six months old (B; $p < 0.001$). Mice were killed by intracardiac perfusion with 4% PFA. Their heart weight was measured, and their normalized heart weight to body weight ratio was determined (heart weight/body weight; C). Mean normalized heart weight was higher in BTBR

mice (A, C; $p < 0.001$). Results from Masson's Trichrome stain reveal no fibrosis (E–L). The cross-sectional area (CSA) revealed larger cardiomyocytes in BTBR mice compared to B6 mice (D; $p < 0.001$), as well as larger CSA in a mismatched LD cycle (D; $p < 0.001$).

Following an insulin bolus, glucose clearance was impaired in mice under mismatched LD cycles (Fig. 5B; main effect of LD cycle; $F_{(1, 74)} = 19.52$, $p < 0.001$, $\omega_p = 0.26$). BTBR mice had a smaller area under the curve (main effect of strain; $F_{(1, 74)} = 4.31$, $p = 0.044$, $\omega_p = 0.06$). Males had impaired responses to insulin compared to females (main effect of sex; $F_{(1, 74)} = 19.65$, $p < 0.001$, $\omega_p = 0.26$). Female BTBR mice were more sensitive to insulin relative to BTBR males and all B6 mice (strain by sex interaction; $F_{(1, 74)} = 8.90$, $p = 0.004$, $\omega_p = 0.13$).

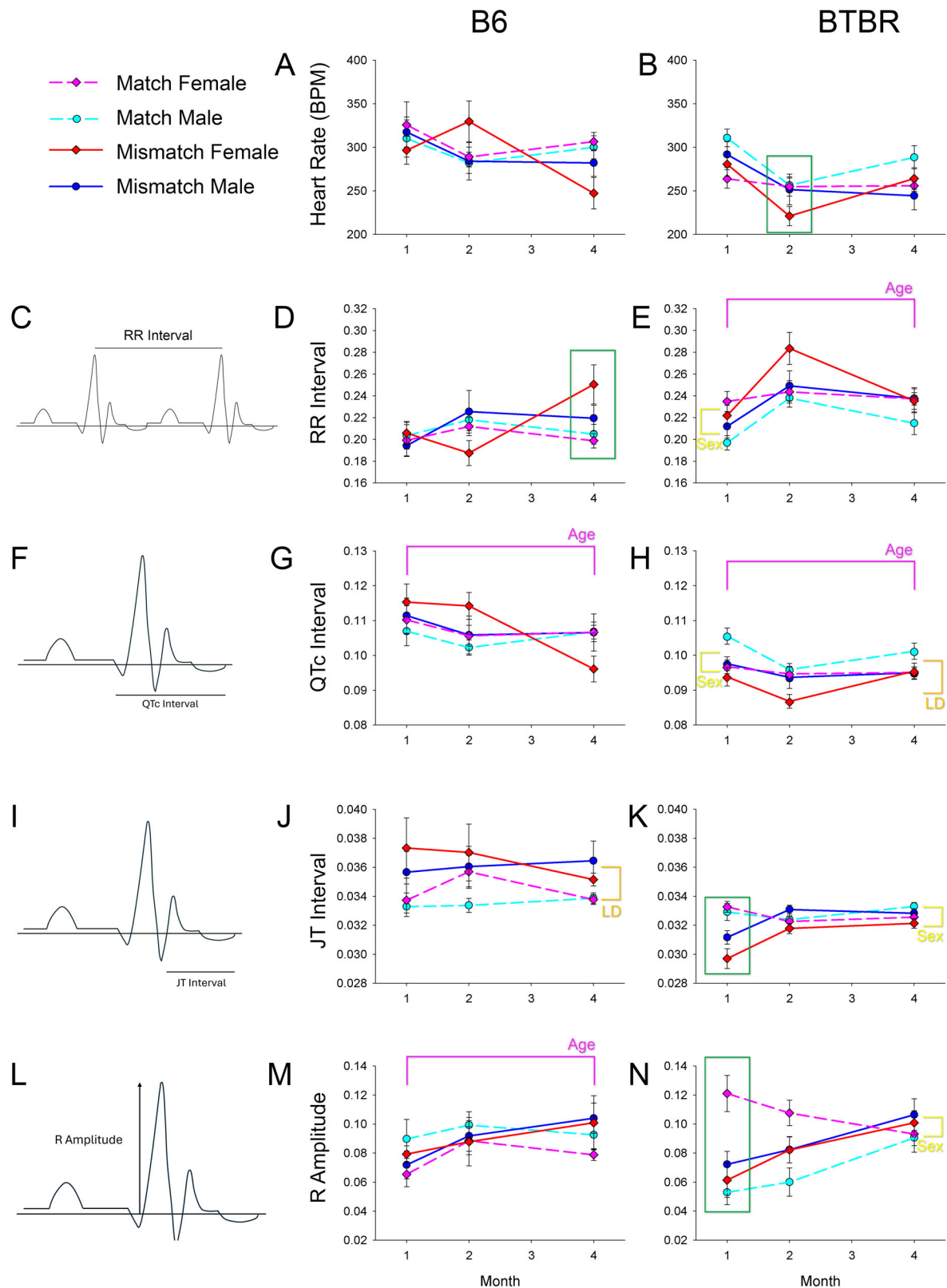
Discussion

The purpose of this study was to better understand how circadian misalignment contributes to early insulin resistance and hypertrophied hearts previously seen in BTBR mice. Further, we sought to explore the onset of cardiometabolic disease in healthy B6 mice gestated and housed in a short LD cycle. The data presented here supports the hypotheses that early life circadian misalignment results in worse cardiometabolic health outcomes in both strains. Results from glucose and insulin tolerance tests reveal that even a small change in LD cycle length (~63–75 min different than endogenous freerunning period) from conception onwards results in early onset insulin resistance in both strains of mice, with males being worse off. Further, both strains experienced changes in cardiac parameters between LD cycles. Most notably, mismatched BTBR mice displayed shorter QTc intervals and slower heart rates, while mismatched B6 mice had prolonged RR and JT intervals. LD cycle did not significantly alter body weight, although both strains of mice tended to be heavier when misaligned. Normalized heart weight was not affected by LD cycle but cardiomyocyte size was increased under a mismatched LD cycle.

Despite their large heart size, the literature on the cardiac function of the BTBR mouse is sparse. We show that BTBR mice do, indeed, have increased normalized heart weight compared to B6 mice. Further, BTBR mice have larger heart cells than B6 mice corresponding to observations of

larger deflections along the cardiac waveform²⁷. Interestingly, mismatched BTBR mice displayed slower heart rates and shortened QTc intervals. Typically, QT intervals are prolonged 2 ms for every 10 ms prolongation of the RR interval²³. This, along with cardiodepressant effects of xylazine, is corrected for using the Bazette correction. Still, we were able to detect shorter QTc intervals in mismatched BTBR mice. Although limited studies have explored short QT syndrome (SQTS) in mice, studies in humans suggest that the failure of QTc intervals to prolong in the presence of bradycardia is associated with SQTS, as well as a family history of sudden death⁴¹, which is commonly observed in BTBR mice. Change in anatomy between LD cycles at six months old and differences in electrophysiology can support worsening of heart function due to chronic exposure to circadian misalignment in this strain during the first four months of life. These differences may become more evident as mice age.

The lack of fibrosis and prolongation of QTc intervals in B6 mice was unexpected given past research that links the circadian system to the cardiovascular system^{13,14}. Martino and colleagues²² observed interstitial fibrosis and cardiac hypertrophy in 17-month-old hamsters housed in misaligned LD cycles that improved when placed back on a matched LD cycle. Similarly, West and colleagues²⁴ observed prolonged PR, QTc and RR intervals in mice raised on a 22.5-h LD cycle from 17 to 52 weeks old, attributed to disrupted autonomic activity. Aging has been shown to lead to progressive fibrosis, characterized by a reduction in cardiomyocytes, an increase in collagen deposits^{42,43}, and prolonged PQ intervals²⁵. Disrupted heart function due to circadian misalignment could depend on aging as past studies using 21-month-old mice with CLOCK gene mutations found age-dependent increases in normalized heart weight, hypertrophy, and impaired contractility¹². Although we observed electrophysiological and metabolic disturbances, changes in cardiovascular anatomy might take longer to develop, as seen in those previous experiments. We monitored the health of our mice up to



6 months old, roughly equivalent to a 20-year-old human. Previous experiments using animal models found heart disease at 17 months old, comparable to that of a 60-year-old human. Aging is associated with cardiac hypertrophy, remodeling, and impaired repair following cardiac injury⁴². Although fibrotic pathways are, in part, regulated by the cardiomyocyte clock, aging exacerbates the decline in heart function and

vice versa, largely through molecular crosstalk between the circadian system and cardiac signaling^{13,42,43}.

On the contrary, profound heart disease has been observed in younger mice (8-week-old) when they were subjected to a more severe form of circadian disruption than what we applied here. Specifically, chronic phase shifting the LD cycle starting during gestation led to disrupted mice showing

Fig. 4 | Changes in cardiac electrophysiological parameters overtime in B6 and BTBR mice between LD cycles. The schematics on the left (C, F, I, L) illustrate the interval or wave amplitude of the respective cardiac parameters being measured in B6 (A, D, G, J, M) and BTBR (B, E, H, K, N) mice on the right. Male (blue) and female (red/pink) B6 and BTBR mice were conceived and housed in a matched (light blue/pink) or a mismatched (dark blue/red) LD cycle until 6 months old. At one, two, and four months old each group received an ECG and their heart rates (A, B), RR (C–E), QTc (F–H), JT (I–K) intervals, and R amplitude (L–N), were compared between groups overtime. BTBR hearts rates significantly differed between one month old and two months old ($p < 0.001$) and one month old and four months old (B;

$p < 0.01$), while RR intervals significantly differed between one month and two months old ($p < 0.001$), one month and four months old ($p < 0.05$), and two months and four months old (E; $p < 0.01$). B6 mice had longer JT intervals (J; $p < 0.01$) and longer RR intervals overtime (D; $p < 0.05$) in the mismatched LD cycle. QTc intervals in BTBR mice were significantly longer between one month old and two months old ($p < 0.001$) and two months old and four months old (H; $p < 0.05$). At one month old, BTBR mice in the 24-h LD cycle had significantly longer JT intervals (K; $p < 0.001$) and significantly longer R amplitudes in females (N; $p < 0.001$). Significant interactions with LD cycle are boxed out in green, main effects of LD cycle, sex, and time are highlighted in orange, yellow, and purple, respectively.

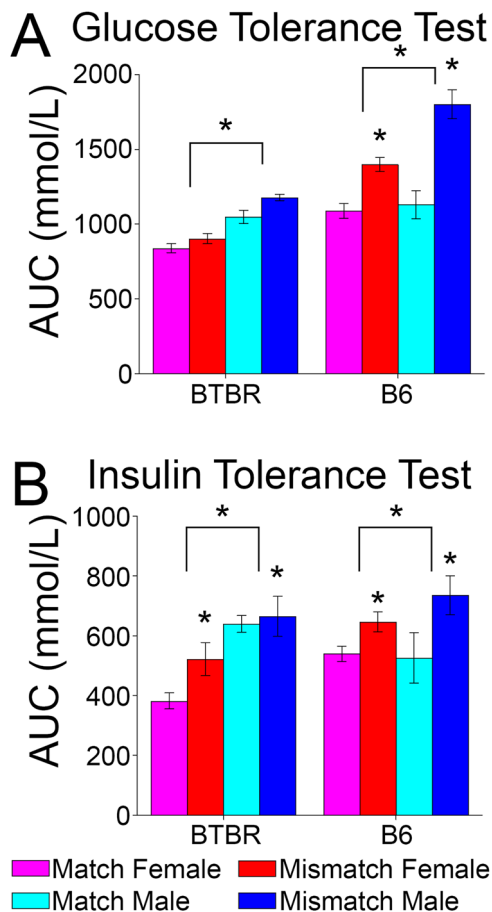


Fig. 5 | Changes in metabolism in B6 and BTBR mice between LD cycles. Blood glucose levels were measured and the area under the curve (AUC) was calculated and compared between groups following the GTT or the ITT. Male B6 mice had the largest area under the curve following administration of 2 kg/g of glucose (A; $p < 0.001$), and mismatched females had significantly larger AUCs than matched females (A; $p < 0.01$). Misaligned male BTBR mice had larger AUCs than females in a misaligned LD cycle following a glucose bolus (A; $p < 0.01$). B6 mice had slightly larger AUCs than BTBRs (B; $p < 0.05$) and males had larger AUCs than females (B; $p < 0.001$). Mismatched B6 and BTBR mice displayed larger AUCs following an injection of 0.75IU/kg of insulin compared to matched groups (B; $p < 0.001$). Error bars represent SEM.

elevated markers of cardiac remodeling, cardiac hypertrophy, and compromised electrophysiology³². The consistent 9-h delay during gestation was thought to be an environmental stressor that could contribute to the pathological cardiac remodeling seen in these young mice, especially given that the circadian system has direct control over stress hormones. In contrast, we used small changes in the LD cycle (63 min) to study disease progression under a mild, but persistent circadian stress. This may have not provided enough stress on B6 mice to observe such changes in anatomy in early life. Our colony of B6 mice already have short FRPs

around 23.8 h³⁶. A difference of ~63 min might not result in the compounding effects of circadian misalignment and stress Yu and colleagues³² paradigm did to elicit cardiac remodeling. Instead, we found prolonged RR and JT intervals in B6 mice in the absence of cardiac hypertrophy or fibrosis.

Differences observed here in electrophysiology could be a response to circadian misalignment that precede remodeling in B6 and BTBR mouse hearts. Indeed, the circadian system regulates cardiac function through cell-autonomous circadian oscillators within cardiomyocytes that lead to time-of-day rhythms in ion channel homeostasis and contractility that are detectable by an ECG^{10,14,44,45}. Mutations in canonical clock genes have been shown to prolong the length of RR and QTc intervals^{14,23}. While changes to the ECG are detectable in these earlier ages, it may require longer for fibrosis to progress to detectable levels. Examining mice housed under our mismatched LD cycles for longer than those examined here might help resolve this question.

Both strains of mice exhibited reduced insulin sensitivity at three months of age when gestated and housed in a mismatched LD cycle. Specifically, mismatched male and female B6 mice experience elevated blood glucose levels following a glucose or insulin bolus relative to their matched counterparts. Past studies found early glucose intolerance in three-month-old female B6 mice gestated and raised in an extremely short (8:8 hr) LD cycle, but not males³¹, while other disruption paradigms did not find heightened blood glucose levels in males or females³². Our results from B6 mice are in line with past findings that suggest circadian dysfunction can increase the risk for diabetes through perturbations in insulin signaling and rhythmic glucose excretion, with males being at greater risk⁴⁰. Since a T-cycle with a period of 16 h would be outside the limits of entrainment, it is possible that the effects observed in the study by Her and colleagues³¹ may have had less to do with misalignment between the internal clock and the LD cycle, but instead could be associated with disorganized behavior that loosely coordinates to the LD cycle. Such an LD cycle would still be disrupting, but likely represents a different experience than the strain of entraining to a LD cycle right at the limit of entrainment.

While a mismatch LD cycle affected all mice in the insulin tolerance test, only the B6 mice were affected by the LD cycle in the glucose test. The GTT measures how well the pancreas is able to compensate for rising glucose levels, either by increasing beta cell mass, or insulin production⁴⁶. Type 2 diabetes is a result of glucotoxicity due to insulin resistance that destroys beta cells, causing the pancreas to decompensate⁴⁷. The BTBRs change in response to the ITT versus the GTT suggests their pre-diabetic phenotype is, in part, affected by the misalignment between the LD cycle and their FRP. However, this is characterized by reduced insulin sensitivity that could eventually lead to glucose intolerance. Taken together, both strains exhibited optimal metabolic functioning under T-cycles that match their endogenous period. This is similar conceptually to competition assays using period mutant cyanobacteria, *Arabidopsis* and some period mutant fruit flies⁴⁸. When many period mutant lines are grown together both the cyanobacteria⁴⁹ and the *Arabidopsis*⁵⁰ lines whose FRP best matched the imposed T cycle outcompeted the other lines. The same was true of long period, but not short period fruit flies⁵¹. This suggest enhanced fitness

resulting from resonance between the circadian period and imposed T-Cycle is a basic principle observable in species across the various Kingdoms of life⁴⁸.

Male and female B6 and BTBRs tended towards heavier body weights in mismatched LD cycles. Although this was previously found following gestational exposure to circadian disruption^{31,32}, other studies found reduced metabolic efficiency characterized by increased food intake and lower body weights in mice housed in a 22.5-h LD cycle for one year, starting at 8 weeks old²⁴. Given that a 22.5-h LD cycle more closely matches our experiment here, apart from gestational exposure, differences could depend on gestational versus adult exposure to circadian misalignment. Tracking the body weight of our animals into late adulthood to observe either maintenance of weight gain or the onset of reduced metabolic efficiency could elucidate this.

As expected, male mice from both strains exhibited a more severe resistance to insulin when misaligned, and higher fasting blood glucose levels compared to females overall. However, cardiac outcomes were similar between sexes. Research indicates that males are more prone to cardiometabolic disease due to higher testosterone and lower estradiol levels^{52,53}. Studies show that increasing testosterone in males and performing ovariectomies in females worsen cardiometabolic outcomes, highlighting the protective role of female sex hormones^{52,53}. Past research found that females are protected against the cardiomyopathic consequences of CLOCK mutations in the cardiomyocyte clock previously seen in males⁵², unlike our study. Discrepancies in findings may stem from variations in the type and timing of circadian disruption⁵⁴. Some studies suggest there is an additive effect, with prenatal, perinatal, and adult exposure resulting in worse outcomes than imposing it on one developmental stage⁵⁴. Considering the circadian disruption paradigm is important for comparing health outcomes between age and sexes.

Our study provides evidence for sex-dependent worsening of cardiometabolic health due to discrete changes in LD cycles in two strains of mice. The circadian misalignment paradigm we introduced here is more comparable to what humans suffering from advanced sleep phase syndrome experience, and is therefore more indicative to what they or their offspring could be susceptible to⁵. Moreover, we show that circadian disruption on its own can lead to cardiometabolic disease in healthy mice and worsen pre-existing disease. This provides support for circadian etiology for increased prevalence of obesity and diabetes in humans that do shiftwork, apart from changes in diet and routine^{7,40}. Future studies should make direct comparisons between cardiometabolic health in young adulthood, middle-age, and old-age, as well as differences between gestational exposure versus exposure in adulthood, to better understand how disease onset and severity is affected by chronic circadian misalignment throughout the lifespan. Elucidating this will further contribute to understanding the relationship between the rise in non-communicable diseases and lifestyles that lead to circadian misalignment in humans.

Methods

Animals

Male and female C57BL/6 (B6; $n = 57$) and BTBR T+Itpr3tf/J (BTBR; $n = 67$) mice were bred in lab from founders originally acquired from the University of Calgary Life and Environmental Science Animal Resource Center and Jackson Laboratories, USA, respectively. Breeders were randomly assigned to either a 12:12 hr (24-h) or a 11.375:11.375 h (22.75-h) LD cycle. Both strains of mice were conceived, gestated, and raised in their respective LD cycle. Sample actograms from adult mice from both strains housed in these LD cycles are presented in Supplementary Figs. 1–3. Mice were weaned on postnatal day 19–21 and housed with 2–5 same sex littermates in polycarbonate cages (28 × 17 × 12 cm) containing woodchip bedding, paper nesting material, and housing enrichment in the form of cardboard houses. Ambient temperature was maintained between 20 and 23 °C and humidity was controlled. Standard laboratory chow and water were available *ad libitum* (Purina Lab Diet 5001). Wheel running data (Supplementary Figs. 1+2) were acquired using non-experimental animals housed in polycarbonate cages (30.3 × 20.6 × 26 cm) and measured using

ClockLab Software (Actimetrics Wilmette, IL, USA). All experiments were conducted between 1 and 6 months old. Experimental procedures were approved by the Life and Environmental Sciences Animal Care Committee at the University of Calgary and were performed in accordance with the guidelines on ethical animal use by the Canadian Council on Animal Care.

Electrocardiogram recordings

ECGs of female and male BTBR mice ($n = 63$) and B6 mice ($n = 45$) LD cycle were recorded at 1-, 2-, and 4-month of age. Mice that died before all three recordings were attained were removed from analysis. To control for circadian influences, ECGs were conducted at the same circadian phase (i.e., 1–3 h after lights on) for each LD cycle^{55,56}. Mice were anesthetized with ketamine (0.1 g/kg) and xylazine (5 mg/kg). Administration of the anesthetic agent per mouse was staggered between each ECG reading⁵⁶. Electrode gel (Spectra 360) was applied to two snap electrodes and placed dorsolaterally above the forelimbs on the either side of the scapula and secured with tape^{25,38}. ECGs were recorded until a clean continuous reading of approximately 40 s was acquired (PowerLab)^{25,27,55}. ECG signals were digitized at a sampling rate of 1000 Hz with a mains filter and a notch filter set to 60 Hz.

Using the ECG module in LabChart7 (ADInstruments), correct identification of each R complex was manually verified²⁵. The average distance between R intervals was automatically calculated (RR interval). The amplitude and frequency of PQRSJT and PR, QRS, QT, and corrected QT (QTc) intervals were defined manually in the averaging view and calculated automatically using Bazette correction under mouse settings^{27,56,57}. The length of the P wave was determined to be between two isoelectric points. The QRS interval was defined as the beginning of the isoelectric point along the Q wave, to the isoelectric point along the J wave, as previously defined^{27,57}. The ST segment was defined as the plateau between the positive J wave deflection and the negative T wave deflection. The end of the T wave was defined as the first plateau between the T wave and the next P wave. Example of wave boundaries are shown in Supplementary Fig. 3. ECG signals were averaged over >100 R complexes²⁶. Given that cardiac function can be affected by bodyweight, we also analyzed the ECG data corrected for bodyweight (Supplementary Fig. 4).

Histology

Mice were weighed and killed at approximately 6 months old by pentobarbital overdose (Euthanyl, 500 mg/kg i.p.) followed by intracardiac perfusion using 4% paraformaldehyde (PFA). Hearts were collected, weighed, and kept in 4% PFA overnight, followed by 30% sucrose with sodium azide until ready for staining. Normalized heart weight was determined by dividing heart weight in grams by body weight in grams. Hearts were cut into 2/3 sagittal sections and embedded in paraffin. A microtome was used to cut slices of heart sections at 5 microns. Masson's Trichrome Stain and Picrosirius Red Stain protocols were performed on slide as per the manufacturer (Sigma Aldrich and abcam, respectively). Tissue processing and staining was performed at an independent site, Health Sciences Center, Foothills Campus (Calgary, AB), Libin Cardiovascular Institute Core Pathology Services. CSA was measured using ImageJ software (NIH, USA). Individual cells were identified and traced. CSA was determined by averaging over 30 cells along the free left ventricular wall.

Intraperitoneal insulin and glucose tolerance tests

Intraperitoneal Insulin Tolerance Tests (ITT; $n = 54$) and Glucose Tolerance Tests (GTT; $n = 59$) were performed at 13 weeks of age. For both tests, animals were placed in a clean cage with a new hopper within 1-h after lights on in their respective LD cycle. Animals fasted throughout the resting period for 6 h. Each cage was randomly assigned to receive an intraperitoneal (IP) injection of either glucose (2 g/kg) or insulin (0.75 IU/kg). Blood glucose levels were collected by lancing the tip of the tail and gently massaging a drop of blood out of the tip. The drop was placed on a testing strip and measured over 5 time points: before IP injection and 15-, 30-, 60-, and 120-min following IP injection. Every subsequent drop at each time point was

massaged out (mice were only lanced once). Blood glucose levels were measured using Freestyle Lite Meter and ZipWik tabs, a device previously used in rodent models⁵⁸. Multiple glucometers of the same brand were compared on testing day and batteries were routinely changed to maintain accuracy of readings. Blood glucose levels were recorded over two hours and the area under the curve (AUC) was used to compare glucose and insulin sensitivity between strains, LD cycles, and sex.

Statistical analysis

Two three-way ANOVAs were performed on each strain to assess differences in the AUC between LD cycle, sex, and strain for GTT and ITT. Two three-way ANOVAs were used to assess the differences between body weight (BW) and normalized heart weight (HW; HW/BW (g/g)) between LD cycles, sex, and strain. A four-way mixed ANOVA was used to investigate changes in body weight over the first four months of life between LD cycle, sex, and strain. One three-way ANOVA was used to investigate differences between strain, LD cycle, and sex in CSA of cardiomyocytes. Five three-way mixed model ANOVAs were used to investigate the difference in the RR interval, heart rate (beats per minute), QTc interval, JT interval, and R wave amplitude. Upon violations to sphericity, Greenhouse-Geisser's adjusted *p*-values are reported. When violations to normality or heterogeneity of variance occur alone, statistical significance is set to *p* < 0.01. Otherwise, results *p* < 0.05 are considered significantly significant. One extreme outlier was removed from histology to correct for violations to both normality and between group variances. Post hoc comparisons were made using Holm's adjustment of *p* values. Analysis was performed using R studio. All statistical tests are summarized in Supplementary Table 1.

Data availability

All numerical data files are available at <http://borealisdata.ca/>. Heart histology slides are available from MCA upon request.

Received: 12 July 2024; Accepted: 5 March 2025;

Published online: 13 May 2025

References

- Lin, X. et al. Global, regional, and national burden and trend of diabetes in 195 countries and territories: An analysis from 1990 to 2025. *Sci. Rep.* **10**, 14790 (2020).
- Roth, G. A. et al. Global burden of cardiovascular diseases and risk factors, 1990–2019: Update from the GBD 2019 study. *J. Am. Coll. Cardiol.* **76**, 2982–3021 (2020).
- Fonken, L. K. & Nelson, R. J. The effects of light at night on circadian clocks and metabolism. *Endocr. Rev.* **35**, 648–670 (2014).
- Giuntella, O. & Mazonna, F. Sunset time and the economic effects of social jetlag: evidence from US time zone borders. *J. Health Econ.* **65**, 210–226 (2019).
- Nobre, B., Rocha, I., Morin, C. M. & Cruz, M. M. E. Insomnia and circadian misalignment: an underexplored interaction towards cardiometabolic risk. *Sleep. Sci.* **14**, 55–63 (2021).
- Rüger, M. & Scheer, F. A. Effects of circadian disruption on the cardiometabolic system. *Rev. Endocr. Metab. Disord.* **10**, 245–260 (2009).
- Ansu Baidoo, V. & Knutson, K. L. Associations between circadian disruption and cardiometabolic disease risk: A review. *Obes. (Silver Spring, Md.)* **31**, 615–624 (2023).
- Wyse, C. A., Selman, C., Page, M. M., Coogan, A. N. & Hazlerigg, D. G. Circadian desynchrony and metabolic dysfunction; did light pollution make us fat? *Med. hypotheses* **77**, 1139–1144 (2011).
- Krittika, S. & Yadav, P. Circadian clocks: an overview on its adaptive significance. *Biol. Rhythm Res* **51**, 1109–1132 (2020).
- Takeda, N. & Maemura, K. The role of clock genes and circadian rhythm in the development of cardiovascular diseases. *Cell. Mol. life Sci. : CMLS* **72**, 3225–3234 (2015).
- Zhang, J., Chatham, J. C. & Young, M. E. Circadian regulation of cardiac physiology: Rhythms that keep the heart beating. *Annu. Rev. Physiol.* **82**, 79–101 (2020).
- Alibhai, F. J. et al. Disrupting the key circadian regulator CLOCK leads to age-dependent cardiovascular disease. *J. Mol. Cell. Cardiol.* **105**, 24–37 (2017).
- El Jamal, N., Lordan, R., Teegarden, S. L., Grosser, T. & FitzGerald, G. The circadian biology of heart failure. *Circul. Res.* **132**, 223–237 (2023).
- Martino, T. A. & Young, M. E. Influence of the cardiomyocyte circadian clock on cardiac physiology and pathophysiology. *J. Biol. Rhythms* **30**, 183–205 (2015).
- Um, J. H. et al. AMPK regulates circadian rhythms in a tissue- and isoform-specific manner. *PLoS One* **6**, e18450 (2011).
- Zeb, F. et al. Time-restricted feeding regulates molecular mechanisms with involvement of circadian rhythm to prevent metabolic diseases. *Nutrition* **89**, 111244 (2021).
- Abbott, S. M. & Zee, P. C. Circadian rhythms: implications for health and disease. *Neurol. Clin.* **37**, 601–613 (2019).
- Costello, H. M. & Gumz, M. L. Circadian rhythm, clock genes, and hypertension: recent advances in hypertension. *Hypertension* **78**, 1185–1196 (2021).
- Fagiani, F. et al. Molecular regulations of circadian rhythm and implications for physiology and diseases. *Signal Transduct. Target Ther.* **7**, 41 (2022).
- Marhefkova, N., Sládek, M., Sumová, A. & Dubsy, M. Circadian dysfunction and cardio-metabolic disorders in humans. *Front. Endocrinol.* **15**, 1328139 (2024).
- Caliandro, R., Streng, A. A., van Kerkhof, L. W., van der Horst, G. T. & Chaves, I. Social jetlag and related risks for human health: A timely review. *Nutrients* **13**, 4543 (2021).
- Martino, T. A. et al. Circadian rhythm disorganization produces profound cardiovascular and renal disease in hamsters. *Am. J. Physiol. Regul. Integr. Comp. Physiol.* **294**, R1675–R1683 (2008).
- Gottlieb, L. A., Larsen, K., Halade, G. V., Young, M. E. & Thomsen, M. B. Prolonged QT intervals in mice with cardiomyocyte-specific deficiency of the molecular clock. *Acta Physiol.* **233**, e13707 (2021).
- West, A. C. et al. Misalignment with the external light environment drives metabolic and cardiac dysfunction. *Nat. Commun.* **8**, 417 (2017).
- Merentie, M. et al. Mouse ECG findings in aging, with conduction system affecting drugs and in cardiac pathologies: Development and validation of ECG analysis algorithm in mice. *Physiol. Rep.* **3**, e12639 (2015).
- Speerschnieder, T. & Thomsen, M. Physiology and analysis of the electrocardiographic T wave in mice. *Acta Physiol.* **209**, 262–271 (2013).
- Sysa-Shah, P., Sørensen, L. L., Abraham, M. R. & Gabrielson, K. L. Electrocardiographic characterization of cardiac hypertrophy in mice that overexpress the ErbB2 receptor tyrosine kinase. *Comp. Med.* **65**, 295–307 (2015).
- Mendez, N. et al. Gestational chronodisruption impairs circadian physiology in rat male offspring, increasing the risk of chronic disease. *Endocrinology* **157**, 4654–4668 (2016).
- Varcoe, T. J., Wight, N., Voultsios, A., Salkeld, M. D. & Kennaway, D. J. Chronic phase shifts of the photoperiod throughout pregnancy programs glucose intolerance and insulin resistance in the rat. *PLoS One* **6**, e18504 (2011).
- Ameen, R. W., Warshawski, A., Fu, L. & Antle, M. C. Early life circadian rhythm disruption in mice alters brain and behavior in adulthood. *Sci. Rep.* **12**, 7366 (2022).
- Her, T. K. et al. Circadian disruption across lifespan impairs glucose homeostasis and insulin sensitivity in adult mice. *Metabolites* **14**, 126 (2024).

32. Yu, Y. et al. Circadian disruption during fetal development promotes pathological cardiac remodeling in male mice. *iScience* **27**, 109008 (2024).
33. Benno, R., Smirnova, Y., Vera, S., Liggett, A. & Schanz, N. Exaggerated responses to stress in the BTBR T+ tf/J mouse: an unusual behavioral phenotype. *Behav. Brain Res.* **197**, 462–465 (2009).
34. Silverman, J. L. et al. Low stress reactivity and neuroendocrine factors in the BTBR T+ tf/J mouse model of autism. *Neuroscience* **171**, 1197–1208 (2010).
35. Zilkha, N., Kuperman, Y. & Kimchi, T. High-fat diet exacerbates cognitive rigidity and social deficiency in the BTBR mouse model of autism. *Neuroscience* **345**, 142–154 (2017).
36. Vijaya Shankara, J., Horsley, K. G., Cheng, N., Rho, J. M. & Antle, M. C. Circadian responses to light in the BTBR Mouse. *J. Biol. Rhythms* **37**, 498–515 (2022).
37. Couderc, J. P. & Lopes, C. M. Short and long QT syndromes: Does QT length really matter? *J. Electrocardiol.* **43**, 396–399 (2010).
38. Calvet, C. & Seebeck, P. What to consider for ECG in mice—with special emphasis on telemetry. *Mamm. Genome* **34**, 166–179 (2023).
39. Chaix, A., Manoogian, E. N. C., Melkani, G. C. & Panda, S. Time-restricted eating to prevent and manage chronic metabolic diseases. *Annu. Rev. Nutr.* **39**, 291–315 (2019).
40. Han, H., Dou, J., Hou, Q. & Wang, H. Role of circadian rhythm and impact of circadian rhythm disturbance on the metabolism and disease. *J. Cardiovasc. Pharm.* **79**, 254–263 (2022).
41. Dewi, I. P. & Dharmadhati, B. B. Short QT syndrome: The current evidences of diagnosis and management. *J. Arrhythm.* **36**, 962–966 (2020).
42. Biernacka, A. & Frangogiannis, N. G. Aging and cardiac fibrosis. *Aging Dis.* **2**, 158 (2011).
43. Kong, P., Christia, P. & Frangogiannis, N. G. The pathogenesis of cardiac fibrosis. *Cell. Mol. Life Sci.* **71**, 549–574 (2014).
44. Bernardi, J., Aromolaran, K. A., Zhu, H. & Aromolaran, A. S. Circadian mechanisms: Cardiac ion channel remodeling and arrhythmias. *Front. Physiol.* **11**, 611860 (2020).
45. Mia, S. et al. Differential effects of REV-ERBa/β agonism on cardiac gene expression, metabolism, and contractile function in a mouse model of circadian disruption. *Am. J. Physiol. Heart Circ. Physiol.* **318**, H1487–H1508 (2020).
46. Hinder, L. M. et al. Dietary reversal of neuropathy in a murine model of prediabetes and metabolic syndrome. *Dis. models Mech.* **10**, 717–725 (2017).
47. Clee, S. M. et al. Positional cloning of Sorcs1, a type 2 diabetes quantitative trait locus. *Nat. Genet.* **38**, 688–693 (2006).
48. Jabbur, M. L., Dani, C., Spoelstra, K., Dodd, A. N. & Johnson, C. H. Evaluating the adaptive fitness of circadian clocks and their evolution. *J. Biol. rhythms* **39**, 115–134 (2024).
49. Ouyang, Y., Andersson, C. R., Kondo, T., Golden, S. S. & Johnson, C. H. Resonating circadian clocks enhance fitness in cyanobacteria. *Proc. Natl. Acad. Sci. USA* **95**, 8660–8664 (1998).
50. Dodd, A. N. et al. Plant circadian clocks increase photosynthesis, growth, survival, and competitive advantage. *Science* **309**, 630–633 (2005).
51. Horn, M. et al. The circadian clock improves fitness in the fruit fly, *Drosophila melanogaster*. *Front. Physiol.* **10**, 1374 (2019).
52. Alibhai, F. J. et al. Female ClockΔ19/Δ19 mice are protected from the development of age-dependent cardiomyopathy. *Cardiovascular Res.* **114**, 259–271 (2018).
53. In Het Panhuis, W. et al. Circadian disruption impairs glucose homeostasis in male but not in female mice and is dependent on gonadal sex hormones. *FASEB J. : Off. Publ. Fed. Am. Soc. Exp. Biol.* **37**, e22772 (2023).
54. Smarr, B. L., Grant, A. D., Perez, L., Zucker, I. & Kriegsfeld, L. J. Maternal and early-life circadian disruption have long-lasting negative consequences on offspring development and adult behavior in mice. *Sci. Rep.* **7**, 3326 (2017).
55. Xing, S. et al. Genetic influence on electrocardiogram time intervals and heart rate in aging mice. *Am. J. Physiol. Heart Circulatory Physiol.* **296**, H1907–H1913 (2009).
56. Ho, D. et al. Heart rate and electrocardiography monitoring in mice. *Curr. Protoc. Mouse Biol.* **1**, 123–139 (2011).
57. Boukens, B. J., Rivaud, M. R., Rentschler, S. & Coronel, R. Misinterpretation of the mouse ECG: ‘musing the waves of Mus musculus’. *J. Physiol.* **592**, 4613–4626 (2014).
58. Morley, L. A., Gomez, T. H., Goldman, J. L., Flores, R. & Robinson, M. A. Accuracy of 5 point-of-care glucometers in C57BL/6J Mice. *J. Am. Assoc. Lab. Anim. Sci. : JAALAS* **57**, 44–50 (2018).

Acknowledgements

This work was funded by a Discovery Grant from the Natural Sciences and Engineering Research Council (NSERC) of Canada to MCA.

Author contributions

J.G. and M.A. wrote the manuscript and designed the study. J.G. and M.W. developed the techniques and executed the experiments. J.G. analyzed the data. J.G. and M.A. prepared the figures. All authors reviewed the manuscript.

Competing interests

The authors declare no competing interests.

Additional information

Supplementary information The online version contains supplementary material available at <https://doi.org/10.1038/s44323-025-00032-6>.

Correspondence and requests for materials should be addressed to Michael C. Antle.

Reprints and permissions information is available at <http://www.nature.com/reprints>

Publisher's note Springer Nature remains neutral with regard to jurisdictional claims in published maps and institutional affiliations.

Open Access This article is licensed under a Creative Commons Attribution-NonCommercial-NoDerivatives 4.0 International License, which permits any non-commercial use, sharing, distribution and reproduction in any medium or format, as long as you give appropriate credit to the original author(s) and the source, provide a link to the Creative Commons licence, and indicate if you modified the licensed material. You do not have permission under this licence to share adapted material derived from this article or parts of it. The images or other third party material in this article are included in the article's Creative Commons licence, unless indicated otherwise in a credit line to the material. If material is not included in the article's Creative Commons licence and your intended use is not permitted by statutory regulation or exceeds the permitted use, you will need to obtain permission directly from the copyright holder. To view a copy of this licence, visit <http://creativecommons.org/licenses/by-nc-nd/4.0/>.

© The Author(s) 2025